



## Regulation of cellular responses to macroporous inorganic films prepared by the inverse-opal method

Toru Orita<sup>a,b,\*</sup>, Masahiro Tomita<sup>a</sup>, Katsuya Kato<sup>c</sup>

<sup>a</sup> Division of Chemistry for Materials, Graduate School of Engineering, Mie University, 1577 Kurimamachiya-cho, Tsu, Mie 514-8570, Japan

<sup>b</sup> Taiyo Kagaku Co. Ltd., 800 Yamada-cho, Yokkaichi, Mie 512-1111, Japan

<sup>c</sup> National Institute of Advanced Industrial Science and Technology, 2266-78, Anagahora, Moriyamaku, Nagoya, Aichi 463-8560, Japan

### ARTICLE INFO

#### Article history:

Received 4 November 2010

Accepted 29 December 2010

Available online 7 January 2011

#### Keywords:

Macroporous film

Pore size

Proliferation

Adhesion

Cell morphology

### ABSTRACT

Regenerative medicine for repairing damaged body tissues has recently become critically important. Cell culture scaffolds are required for the control of cell attachment, proliferation, and differentiation in *in vitro* cell cultures. A new strategy to control cell adhesion, morphology, and proliferation was developed by culturing mouse osteoblast-like MC3T3-E1 cells on novel cell culture scaffolds fabricated using ordered nanometer-sized pores (100, 300, 500, and 1000 nm).

Results of this study indicate that after 72 h of incubation, the number of cells cultured on a silica film with a pore size of 1000 nm was similar to or slightly lower than that cultured on a non-porous control silica film. Films with 100–500 nm pore sizes, however, resulted in the cell growth inhibition. Morphology of the cultured cells revealed increased elongation and the formation of actin stress fibers was virtually absent on macroporous silica films with 100–500 nm pore size. Vinculin molecules expressed in cells cultured on the non-porous silica films showed many clear focal adhesions, whereas focal contacts were insufficiently formed in cells cultured on macroporous films. The influence of hydroxyapatite (HAp) and alumina scaffolds on the behavior of MC3T3-E1 cells was also evaluated. The proliferation rate of MC3T3-E1 cells cultured on HAp films with 1000 nm pore size was increased to approximately 20% above than that obtained of cells cultured on non-porous HAp films. These results demonstrate that the pore size and constituents of films play a role in controlling the morphology and proliferation rate of MC3T3-E1 cells.

© 2011 Elsevier B.V. All rights reserved.

### 1. Introduction

The interactions between cells and solid surfaces are crucial to several biological phenomena and a wide variety of biomaterials. Since cells are inherently sensitive to their surroundings, the performance of biomaterials strongly depends on their initial interaction with their biological environment. Thus, surface properties of biomaterials are associated with cell adhesion and subsequent cell behaviors, such as proliferation, migration, cytoskeletal arrangement, differentiation, and apoptosis [1–7]. Understanding the mechanisms whereby cells sense and respond to chemical, physical, and biological signals from material surfaces will facilitate the development of novel biomaterials for the control of cell behavior. These factors are crucial in the fields of tissue engineering, drug development, and regenerative medicine.

Cells have been found to respond differently to smooth surfaces compared to surface made of materials with micro- or nano-scale roughness [8–12]. Several techniques have been explored to create micro- and nano-scale topographies on surfaces, including lithography, chemical and plasma etching, grit blasting, and plasma spraying [13–16]. Although the effects of nano- and micro-patterned topographies on cell responses have been well documented, the mechanisms behind these effects remain unresolved. The effects of nano-scale roughness on the behavior of osteoblast-like MC3T3-E1 cells have been previously reported; reduced differentiation and mineralization in these cells was caused by initial cellular responses dependent on surface roughness, resulting in poor intercellular communication [17].

Cells in their natural environment are surrounded by nanostructures, and form biomolecules that configure themselves into different geometrical arrangements (macropores, nanofibers, and nanocrystals). Therefore, nanopatterned substrates, which have an ordered structure, are potential scaffolds as biomimetic materials. To date, fabrication of micropatterned surfaces has been used in to ordered tissue engineering [18–22]. Recent work by Fukuhira et al. [23] showed that macroporous structures (5 μm) remain spherically shaped and produce abundant extra-cellular matrix

\* Corresponding author at: Division of Chemistry for Materials, Graduate School of Engineering, Mie University, 1577 Kurimamachiya-cho, Tsu, Mie 514-8570, Japan. Tel.: +81 59 231 9428; fax: +81 59 231 9430.

E-mail address: [nqj45366@nifty.com](mailto:nqj45366@nifty.com) (T. Orita).

(ECM) for chondrocytes, and these macroporous structures have the potential to provide chondrocytes with a suitable environment for developing a spherical shape. On the other hand, little information is available concerning ordered macroporous surfaces (100–1000 nm) and their role in cell scaffolds. The inverse opal method, which is a fabrication method used to prepare ordered macroporous films, has been reported in literatures [24–26]. This method uses a glass substrate that is vertically dipped into a polystyrene (PS) bead dispersion and is then slowly withdrawn from the dispersion. Substrate frame solutions, such as silica, HAp, or alumina precursors, are dip-coated around the PS films, and PS templates are removed by simply immersing the films in toluene. Macroporous films are typically used with photographic materials and electrochromic devices but to the best of the currently available knowledge, there is no known application of macroporous films for the development of biomaterials.

This study demonstrates a new method for the nanoscale engineering of the biomaterial surface. Here an assembly of ordered macropore films (pore sizes of 100–1000 nm) was employed to biomimetic materials. The influence of pore size on the proliferation, morphology, and cytoskeleton of MC3T3-E1 cells was examined using fluorescent methods. Furthermore, to determine how cells adhere to a macroporous film, focal adhesions and cell pseudopods on the films were examined by immunofluorescence analysis for vinculin molecules and a field-emission scanning electron microscope (FE-SEM). In addition, the influence of different compositions of macroporous scaffolds was investigated by culturing the cells on macroporous films made of silica, HAp, and alumina macroporous films.

## 2. Experimental

### 2.1. Materials

All materials were of analytical grade and were used as they were received from the manufacturer without any further purification. Mouse osteoblast-like MC3T3-E1 cells (RCB1126) were obtained from RIKEN, Japan. 4', 6-Diamidino-2-phenylindole dihydrochloride (DAPI dihydrochloride, Cat. No. D8417) and monoclonal anti-vinculin antibodies produced in mouse (V9131) were purchased from Sigma–Aldrich (St. Louis, MO, USA). Phosphoric acid, calcium nitrate, citric acid, and aluminum isopropoxide were procured from Wako Pure Chemical Industries, Japan. Tetraethoxysilane (TEOS) was obtained from Shin-Etsu Chemical Co., Japan. Sulfate-modified PS beads (particle sizes 100 nm [S37204], 300 nm [S37492], 500 nm [S37494], and 1000 nm [S37498]), rhodamine phalloidin (R415), and alexa fluor 488 goat anti-mouse IgG antibodies (H+L) (A11029) were obtained from Invitrogen Ltd. (Carlsbad, CA, USA). LIVE/DEAD double staining kit (QIA76) was obtained from Merck, Germany. Immunohistochemistry reagent (434980) was obtained from Thermo Shandon (Pittsburgh, PA, USA). Blocking reagent peroxidase stabilizer-H100 (S410-040.11) was obtained from NOF Co., Japan. The cell proliferation enzyme-linked immunosorbent assay (ELISA) system (RPN250) was obtained from GE Healthcare Co., Japan. This system is based on the measurement of the amount of 5-bromo-2'-deoxyuridine (BrdU) incorporated into proliferating cells during DNA synthesis.

#### 2.1.1. Synthesis of macroporous silica films

Polystyrene (PS) bead films were coated on cover-slip substrates (20 mm × 20 mm) by the dip coating method using a Nano dip coater (SDI, Inc., Japan). The substrates were washed with acetone for 1 h and were treated by a vacuum ultraviolet (VUV) cleaner (UER20.172A; Ushio Inc., Japan) before use. The substrates

were vertically dipped into a 1 wt% (100, 300, and 500 nm) or 2 wt% (1000 nm) PS bead dispersion were withdrawn at a rate of 0.2  $\mu\text{m s}^{-1}$  to form the closed-packed PS bead array. After air drying, the array was heated at 80 °C for 1 h to stabilize the films to some extent. A silica frame solution was synthesized by stirring a mixture of TEOS, EtOH, H<sub>2</sub>O, and 10 M HCl at room temperature for 2 h. The initial molar ratio was TEOS/EtOH/H<sub>2</sub>O/HCl = 1:15:37:0.15. PS films were vertically dipped into the mixture for 20 min and withdrawn at a rate of 0.5  $\text{mm s}^{-1}$  to form silica frames around the PS beads, and were then air dried to promote further polycondensation. PS bead templates were removed by simply immersing the films in toluene overnight, and thereby, yielding the macroporous silica films. After washing and cleaning the cover-slips using a similar method, the cover-slips were vertically dipped into the silica frame solution for 20 min and withdrawn at a rate of 0.5  $\text{mm s}^{-1}$ , thereby resulting in the formation of non-porous silica film.

#### 2.1.2. Synthesis of amino-group-modified macroporous silica films

The pores of the macroporous silica films (300 and 1000 nm) were synthesized using the same procedure that was used in Section 2.1. The macroporous silica films were slowly stirred into a mixture of 30  $\mu\text{l}$  N-(6-aminohexyl)aminopropyltrimethoxysilane and 300  $\mu\text{l}$  toluene at room temperature for 12 h. After removing the solution, the resulting products were dried under N<sub>2</sub> at atmospheric pressure for 12 h.

#### 2.1.3. Synthesis of macroporous hydroxyapatite (HAp) and alumina films

HAp macroporous films were prepared according to a previously described method [27]. PS bead (1000 nm) films were fed by a method similar to that used for the macroporous silica films described above. The HAp frame solution was synthesized by stirring a mixture of H<sub>3</sub>PO<sub>4</sub>, CaNO<sub>3</sub>·(4H<sub>2</sub>O), and H<sub>2</sub>O at room temperature for 2 h. The initial molar ratio was H<sub>3</sub>PO<sub>4</sub>/CaNO<sub>3</sub>·(4H<sub>2</sub>O)/H<sub>2</sub>O = 1:2:0.5. The PS film was vertically dipped into the mixture for 20 min and withdrawn at a rate of 0.5  $\text{mm s}^{-1}$  to form a HAp frame around the PS beads. The resulting product was dried at 80 °C for 1 h and then at room temperature for 24 h *in vacuo*. After removing the PS templates using the same procedure that was used for the macroporous silica film, the film was heated to 550 °C (at a rate of: 1 °C min<sup>-1</sup>) in air and kept at that temperature for 4 h. After washing the cover-slips using a similar method, these cover-slips were vertically dipped in the HAp frame solution for 20 min and withdrawn at a rate of 0.5  $\text{mm s}^{-1}$ . The films were then dried using the same method described previously, thereby, resulting in the formation of non-porous HAp films.

The PS bead (500 nm and 1000 nm) films were formed using a method similar to the above mentioned method to form the macroporous silica films. The solution for the alumina frame was synthesized by stirring a mixture of Al[OCH(CH<sub>3</sub>)<sub>2</sub>]<sub>3</sub>, citric acid, H<sub>2</sub>O, EtOH, and 10 M HCl at room temperature for 2 h. The initial molar ratio was Al[OCH(CH<sub>3</sub>)<sub>2</sub>]<sub>3</sub>/citric acid/H<sub>2</sub>O/EtOH/HCl = 1:0.26:13.9:36.5:3.9 [28]. PS films were vertically dipped in the mixture for 20 min and withdrawn at a rate of 0.5  $\text{mm s}^{-1}$  to form an alumina frame around the closed-packed PS bead array. The drying of the hybrid films and the removal of the PS templates were accomplished using the same methods used for the macroporous HAp films. After washing the cover-slip by a similar method, they were vertically dipped in the alumina frame solution for 20 min and withdrawn at a rate of 0.5  $\text{mm s}^{-1}$ . The films were dried by the same methods as the HAp films, and the non-porous alumina films were obtained.

## 2.2. Characterization of materials

Field-emission scanning electron microscopic (FE-SEM) observations were performed using a Hitachi S4300 microscope at an accelerating voltage of 10 kV. Before the observation, the samples were coated with platinum by sputtering using a Hitachi E-1020 ion sputter. Water contact angles on the films were measured using a DM-50.1 (Kyowa Interface Science, Japan). Fluorescence was measured using a Wallac 1420 ARVOsx multi-counter (Perkin-Elmer). The amount of newly synthesized, BrdU-labeled DNA was detected using an immunoassay at an absorbance of 450 nm.

## 2.3. Cell culture

Mouse osteoblast-like MC3T3-E1 cells were cultured in minimum essential alpha medium ( $\alpha$ -MEM; Invitrogen) supplemented with 10 wt% fetal bovine serum (Invitrogen) and 1 wt% penicillin–streptomycin (Invitrogen). The medium was changed every 2–3 days. Cell culture was maintained in a gas jacket incubator equilibrated with 5% CO<sub>2</sub> at 37 °C. Confluent MC3T3-E1 cells were trypsinized and a suspension of  $0.30 \times 10^5$  to  $2.5 \times 10^5$  cells mL<sup>-1</sup> was added to each film. The films were incubated under standard culture conditions (37 °C, 5% CO<sub>2</sub>). In these experiments, non-porous silica, HAp, and alumina films served as controls.

## 2.4. Cell viability and proliferation

The LIVE/DEAD double staining kit was used for quantifying the viability of cells adhered onto each film. Each film was placed into the wells of 6-well plate. Cell dispersion solution (3 mL,  $0.5 \times 10^5$  cells mL<sup>-1</sup>) was seeded on each film and the plates were incubated for 24 or 72 h under standard cell culture conditions (37 °C, 5% CO<sub>2</sub>). Each film was gently washed twice with phosphate-buffered saline (PBS (-)), and then 600  $\mu$ l LIVE/DEAD double staining reagent was aseptically added to each well. Immediately after the addition of the LIVE/DEAD double staining reagent, the samples were incubated for 15 min. The cells were stained with Cyto dye, a cell-permeable green fluorescent dye for live cells, and propidium iodide (PI), a non-cell-permeable red fluorescent dye for dead cells. Next, the solution was gently aspirated into each well, and was washed with PBS (-). The immunohistochemistry staining solution was added to each film sample. Stained specimens were immediately observed using a fluorescent microscope with a band-pass filter.

## 2.5. Observed cell proliferation using BrdU method

Immunocytochemical detection of the amount of 5-bromo-2'-deoxyuridine (BrdU) incorporated into the newly synthesized DNA was performed by quantifying the amount of adherent cell proliferation that occurred on each film. Films were placed into the wells of a 6-well plate. 3 mL ( $0.5 \times 10^5$  cells mL<sup>-1</sup>) of cell dispersion solution was seeded onto each film and incubated for 24 or 72 h under standard cell culture conditions (37 °C, 5% CO<sub>2</sub>). Detection of BrdU by enzyme-linked immunosorbent assay (ELISA) was performed according to the manufacturer's instructions.

## 2.6. Fluorescent dye for the detection of actin filaments

Films were placed into the wells of a 6-well plate. 3 mL ( $0.15 \times 10^5$  cells mL<sup>-1</sup>) of the cell dispersion solution was seeded onto each film, and the plates were incubated for 24 h under standard cell culture conditions (37 °C, 5% CO<sub>2</sub>). After incubation, the culture medium was removed, and the cells were rinsed with PBS (-) and fixed with 3.7% formaldehyde in PBS (-) for 20 min. Fixed cells were permeabilized with 0.1% Triton-X100 in PBS (-) at room temperature for 5 min and then incubated with 10  $\mu$ l

rhodamine–phalloidin and 400  $\mu$ l PBS (-) for 20 min to label the actin filaments. Furthermore, the cells were incubated with 400  $\mu$ l of diamidino-2-phenylindole (DAPI) in PBS (-) for 20 min to stain cell nuclei. After adding staining solution used for immunohistochemistry analysis, the stained cells were observed using the fluorescent microscope.

## 2.7. Immunofluorescence of vinculin focal adhesions

Films for vinculin staining were prepared by placing it into the wells of a 6-well plate. 3 mL ( $0.1 \times 10^5$  cells mL<sup>-1</sup>) of cell dispersion solution was seeded onto each film. The cells were incubated on each film for 48 h after seeding. The cells were then washed twice before fixation in -20 °C methanol at room temperature for 15 min, and then washed thrice with 10 mM glycine in PBS (-) (PBS-G) to remove excess methanol. Fixed samples were first permeabilized with 2 mL 0.1% Triton-X100 in PBS (-) at room temperature for 5 min and washed once with PBS-G. To reduce nonspecific background staining, the samples were blocked overnight using 2 mL blocking reagent H100. After overnight blocking, the blocking reagent was aspirated and samples were washed thrice with PBS-G. Furthermore, cells were incubated with 200  $\mu$ l monoclonal mouse anti-human vinculin antibodies (1:1000 dilution) in PBS (-) for 60 min. Samples were then washed five times with PBS-G and incubated with 200  $\mu$ l Alexa Fluor 488 goat-anti-mouse IgG secondary antibodies (1:1000 dilution) in PBS (-) for 60 min. Samples were washed five times with PBS-G, then imaged on a fluorescent microscope using FITC filters.

## 2.8. Observations of cell pseudopods using FE-SEM

To clarify how cells adhere to each film, the pseudopods of the cells were observed using FE-SEM. The films were placed into the wells of a 6-well plate. 3 mL ( $0.15 \times 10^5$  cells mL<sup>-1</sup>) of cell dispersion solution was seeded onto the films and incubated for 24 h under standard cell culture conditions (37 °C, 5% CO<sub>2</sub>). The films were then gently washed twice with PBS (-), 3 mL glutaraldehyde (2.5%) in PBS (-) was added to cells, and the mixture was stored at 4 °C for 40 min to fix the cells. The samples were dehydrated by soaking in graded ethanol concentrations (25, 50, 70, 90, and 100%) for 10 min and by immersing them twice in 3 mL hexamethyldisilazane for 5 min. The samples were then coated with platinum by sputtering using the Hitachi E-1020 ion sputter. The pseudopods of the cells were observed using FE-SEM.

## 2.9. Observation of cell morphology by scanning probe microscopy (SPM)

To estimate the height and roughness of the cells that adhered to the macroporous silica film, non-porous silica film, and cover-slips, the cells were observed using SPM. The cells were cultured and dried using the same methods as observations of cell pseudopods using FE-SEM section. The cell morphology was observed using SPM after removing the solution. SPM (SII-NT, SPA400) was set to the dynamic force microscope (DFM) mode (tapping mode) using a Si microcantilever (Si-DF20) with a constant force of 1.3 N m<sup>-1</sup>. Square images of 100  $\mu$ m  $\times$  100  $\mu$ m were obtained at a scanning rate of 2 Hz.

# 3. Results and discussion

## 3.1. Characterization

The structures of the films were monitored using FE-SEM. The films after treatment with toluene showed ordered arrays of spher-

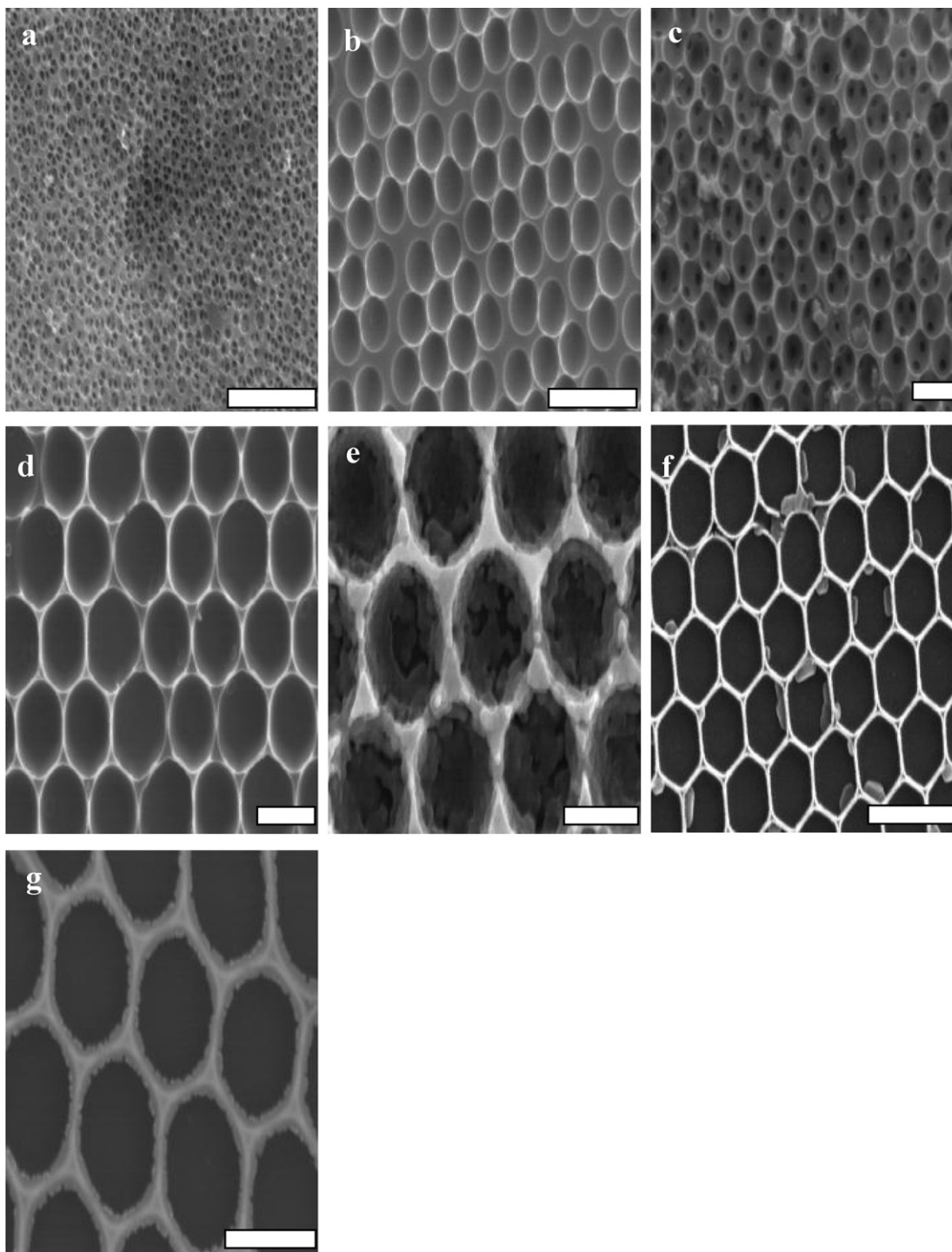


**Fig. 1.** FE-SEM images of the films after removal of the PS template. (a)–(d) show macroporous silica films. (a) Pore size 100 nm, (b) pore size 300 nm, (c) pore size 500 nm, (d) pore size 1000 nm, (e) HAp films with pore size 1000 nm, (f) alumina films with pore size 500 nm, and (g) alumina films with pore size 1000 nm. Scale bar: 1000 nm.

ical macropores formed by the removal of the closed-packed array of polystyrene (PS) beads (Fig. 1). Pore diameters of the macroporous silica films—connected to each other through small windows that are 40–100 nm in diameter—were 100 nm, 300 nm, 500 nm, and 1000 nm. In addition, an SEM image of the macroporous HAp films prepared using the 1000 nm PS template showed a well-ordered 1000 nm pore. SEM images of macroporous alumina films revealed a well-arranged hexagonal lattice with pore sizes of 500 nm and 1000 nm on the surface, which is similar to particle sizes of the PS template.

From the results of contact angle measurements of macroporous silica films, it was determined that the wettability of the surface changes depending on pore size (Fig. 2). These results were compared to those obtained using macroporous silica and non-porous silica films. The measured contact angle was approximately  $100^\circ$  for macroporous silica films with pore sizes 100, 300, and 500 nm, and was considerably higher than a contact angle of  $16.9^\circ$  measured for the non-porous silica films. The water contact angle for macroporous silica films with a pore size of 1000 nm became slightly smaller; contact angle of  $65.7^\circ$  was recorded. These observations

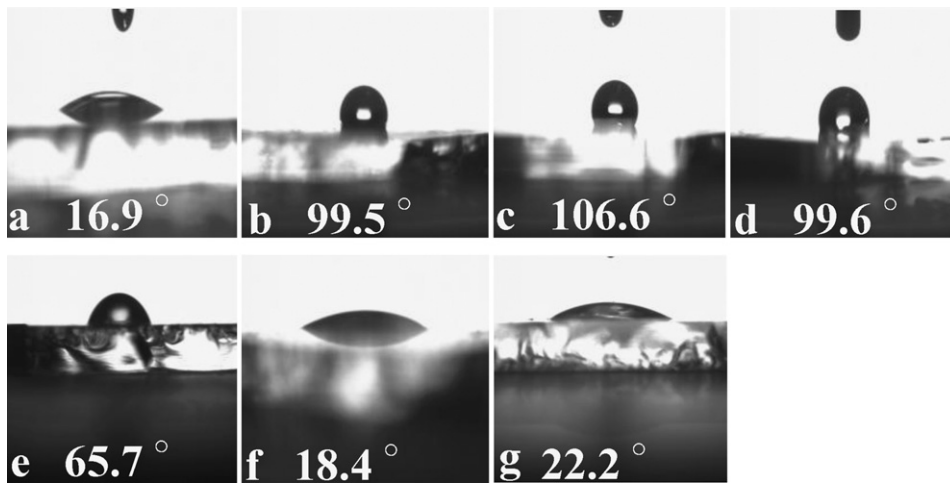


**Fig. 2.** Contact angles of macroporous silica films and amino-group-modified macroporous silica films. (a) Non-porous silica films, (b) pore size 100 nm, (c) pore size 300 nm, (d) pore size 500 nm, (e) pore size 1000 nm, (f) amino-group-modified macroporous silica films pore size 300 nm, and (g) amino-group-modified macroporous silica films pore size 1000 nm.

indicate that macroporous silica films with a pore size of 100 nm, 300 nm, and 500 nm can retain high hydrophobic properties. The formation of pores on the macroporous silica films can be assumed to contribute to the properties of the hydrophobic environment.

The wettability of macroporous silica films with pore sizes 300 and 1000 nm were shown to markedly decrease from 106.6° to 18.4° and 65.7° to 22.2°, respectively, by functionalization with amino groups on the silica frames (Fig. 2). All other films composed of

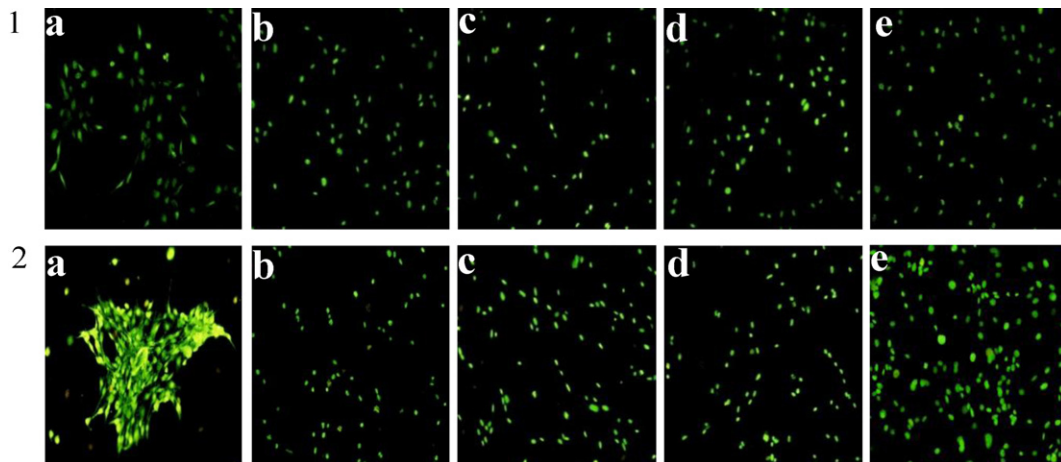


**Fig. 3.** (1) Evaluation of adherent cell viability on macroporous silica films by staining with Cyto dye, a cell-permeable green fluorescent dye for live cells, and PI, a non-cell-permeable red fluorescent dye for dead cells. Cell culture was performed for 24 h (A) and 72 h (B). (a) Non-porous silica films, (b) pore size 100 nm, (c) pore size 300 nm, (d) pore size 500 nm, and (e) pore size 1000 nm. (2) MC3T3-E1 cells proliferation cultured on macroporous silica films. After the cells were stained by the same method described in Section 2.4, cell numbers (density), which are represented as values per unit area, were evaluated using ImageJ software. The error bars indicate the standard deviation ( $n = 3$ ).

macroporous HAp, macroporous alumina, and non-porous materials demonstrated high hydrophilic properties with contact angles of less than  $10^\circ$  (data not shown).

### 3.2. Cell behavior on macroporous silica films

#### 3.2.1. Cell proliferation

Fig. 3(1) and (2) shows cell viability and proliferation after 24 h and 72 h of cultivation, respectively. Cell densities on all surfaces were almost similar after 24 h, suggesting that the macroporous silica films did not adversely affect the initial attachment of these cells. Cell viability was determined by green staining for living cells and red for dead cells during culture periods of 24 h and 72 h, few dead cells were found. Consequently, the cell viability of long-term cultures on macroporous silica films was assumed to be perfect. As for macroporous silica films with pore sizes 100, 300, or 500 nm, the cell proliferation rate observed on these films was approximately 58% lower than that observed on the non-porous, control, silica films. In contrast, as can be seen in Fig. 3(1)-(e) and (2), the number of cells on the 1000 nm silica films showed only a 14% decrease in growth compared to the non-porous silica films. These results suggest that MC3T3-E1 cells can only respond to submicron-scaled pore sizes.

To determine the cell proliferation rate, the amount of BrdU incorporated during DNA synthesis of proliferating cells was evaluated (Fig. 4). The O.D. values which were measured in the cell culture after 24 h on all silica films were 0.13–0.15. Because there were few differences, almost the same number of living cells grew on each film after 24 h of cultivation. After a culture period of 72 h, O.D. values revealing the amount of newly synthesized DNA on the non-porous silica, film and 100, 300, 500, and 1000 nm pore sized macroporous silica films increased by 2.0-, 1.5-, 1.4-, 1.1-, and 1.7-fold, respectively. These results indicate that 100–500 nm nanosized, ordered, silica structures play pivotal roles in controlling the proliferation of MC3T3-E1 cells. This could be attributed to regulation of cell proliferation by controlling the migration capabilities of adherent cells on structures with smaller pore sizes.

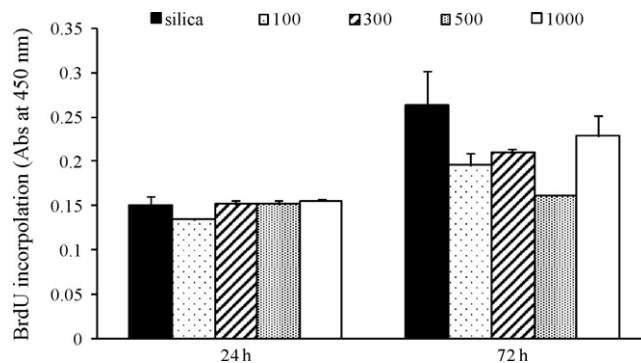


Fig. 4. Assessment of MC3T3-E1 cells proliferation by measuring the amount of BrdU incorporated into newly synthesized DNA at 24 h and 72 h after plating onto the macroporous and non-porous silica films (100–1000 nm). The incorporated BrdU labeling was detected using an immunoassay at an absorbance of 450 nm.

#### 3.2.2. Cell morphology and adhesion behaviors

Fig. 5 shows fluorescent micrographs of actin stress fibers in cells on macroporous silica and non-porous, control, silica films. The cells cultured on the non-porous silica films formed spheroid-like structures, which have a three-dimensional cell aggregation [Fig. 5(a)]. Moreover, cultured cells spread in a planar shape and the formation of actin stress fibers were clearly observed inside cells on the non-porous silica films. This result shows that MC3T3-E1 cells were highly activated with a strong adhesion to the flat substrate. In contrast, adherent cells showed an elongated shape, and actin stress fibers were only slightly visible inside cells on the macroporous silica films. Furthermore, the average cell size on the macroporous silica film was approximately  $5 \mu\text{m} \times 160 \mu\text{m}$  which was smaller than that on the non-porous silica film (approximately  $30 \mu\text{m} \times 40 \mu\text{m}$ ). Because MC3T3-E1 cells generally proliferate with a square shape when cultured on non-porous silica films [29], the change to such an elongated shape is interesting.

To clarify the observed differences in cell adhesion between these films, vinculin, which is expressed as a membrane-

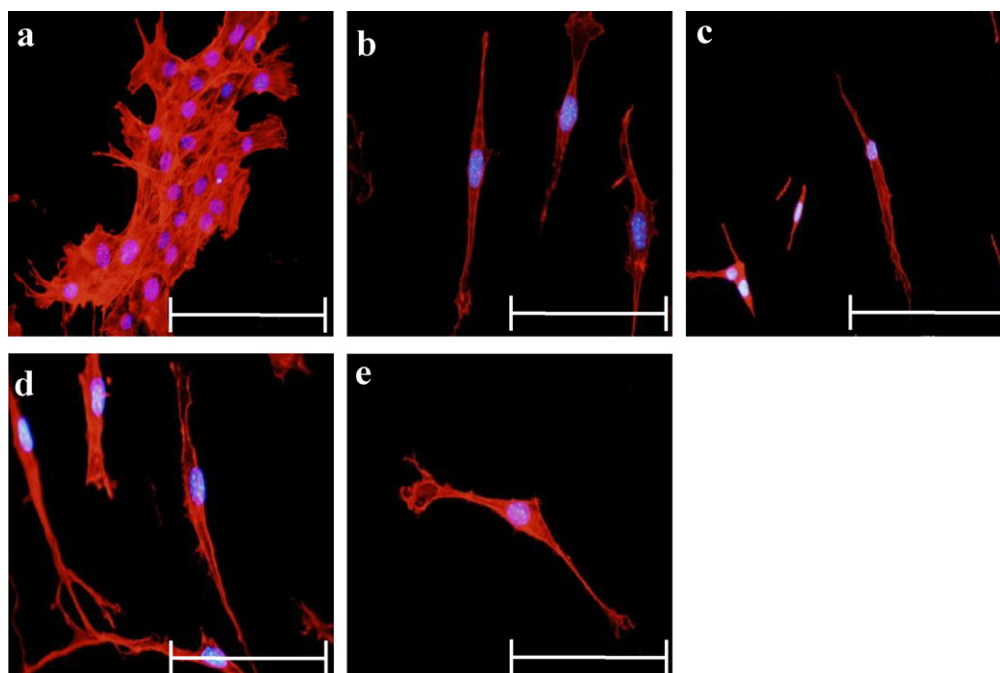
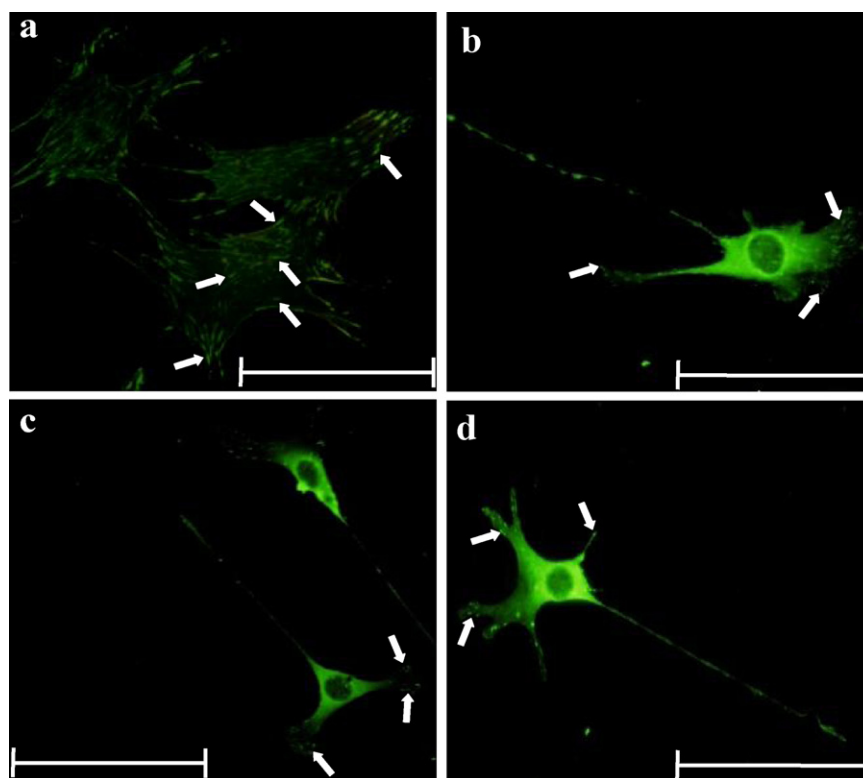


Fig. 5. Fluorescent microscopic images of the F-actin of cells adhered to silica substrates. Cell nuclei are immunostained in blue and actin fibers are stained in red. (a) Non-porous silica films, (b) pore size 100 nm, (c) pore size 300 nm, (d) pore size 500 nm, and (e) pore size 1000 nm. Scale bar:  $100 \mu\text{m}$ . (For interpretation of the references to color in this text, the reader is referred to the web version of this article.)



**Fig. 6.** Immunofluorescent staining of vinculin focal adhesion of a MC3T3-E1 cell adhered to silica substrates. (a) Non-porous films, (b) pore size 300 nm, (c) pore size 500 nm, and (d) pore size 1000 nm. Arrow heads in panels a, b, c, and d indicate vinculin focal adhesion of MC3T3-E1 cells to the silica substrates. Scale bar: 100  $\mu\text{m}$ .

cytoskeletal protein in focal adhesion plaques on films, was stained using the previously described immunofluorescence method. Fig. 6(a) shows that after 48 h of culturing, assembled vinculin was randomly observed in all cell bodies, and focal adhesions were strongly evident on non-porous silica films. On the other hand, few focal adhesions were recognized where the assembled vinculin formed at the tip of the pseudopods of cells on macroporous silica films [Fig. 6(b)–(d)].

An important issue in cell adhesion is the formation of focal adhesions. Without adhesion, osteoblast cells cannot spread [30] and vinculin is required to form a strong actin network. Therefore, these results suggest that macroporous silica structures result in the reduction of attachment points, and that the formation of a distinctive actin cytoskeleton for MC3T3-E1 cells provide MC3T3-E1 cells with a suitable environment for developing an elongated shape. These changes in the cell morphology and adhesion influenced by macropores are presumed be related to regulation of cell proliferation, which is caused by a decrease in the formation of intense cell–cell contacts. These findings support recent reports that indicate that cells react sensitively to nanoscale roughness of silica substrates [31–33].

More precise FE-SEM images of the interactions between cells and macroporous silica films are shown in Fig. 7. The cells on macroporous silica films with a 1000 nm pore size show two different characteristics. First, the pseudopods spread by covering the surface of the macropores of the films [Fig. 7(b)–(2)]. Second, the pseudopods of the cells can grow along the ridge of the macroporous silica scaffold [Fig. 7(b)–(3)]. However, on non-porous, control silica films several pseudopods present so that the cells could gain a rigid adherence [Fig. 7(a)].

Cell morphologies vary greatly on macroporous and non-porous silica films, and this was determined based on the evaluation of actin stress fibers and FE-SEM observations. Next, the observation that the height and roughness of cells affect the adherence

of the cells to a macroporous and non-porous silica films were evaluated using SPM (Fig. 8). Maximum differences in height and peak-to-valley (p–v) values were used as an index for the morphology of cells on macroporous silica films, non-porous silica films, and cover-slips. The p–v value of the cell, which spreads over every direction of the cover-slip, was 1.87  $\mu\text{m}$ ; this value of cells on macroporous and non-porous silica films was approximately 4.50  $\mu\text{m}$ . These results indicate that the bulky structure of the cells was caused by regulation of the cell spreading over macroporous silica films or by three-dimensional cell aggregation on non-porous silica films.

### 3.3. Cell behavior on amino-group-modified macroporous silica films

The influence of the contact angle of macroporous films on cell adhesion and proliferation was evaluated by culturing MC3T3-E1 cells on amino-group-modified, hydrophilic, macroporous silica films prepared by surface functionalization with the silane coupling reagent *N*-(6-aminohexyl)aminopropyltrimethoxysilane. Contact angles of the amino-group-modified macroporous silica films with pore sizes of 300 nm and 1000 nm were markedly decreased from 106.6° to 18.4° and 65.7° to 22.2°, respectively (Fig. 2).

Viability and proliferation of these cells were investigated using the LIVE/DEAD double staining method as described earlier. After 72 h, no dead cells were observed on any films (Fig. 9), indicating that long-term cell culture is possible on amino-group-modified macroporous silica films. However, the number of proliferated cells on macroporous films with a 300 nm pore size decreased by approximately 73% compared to that on non-porous silica films after 72 h of culturing. The increasing number of cells on the 1000 nm macroporous silica films was almost equal to that observed on non-porous silica films. These results demonstrate that the tendency of cell growth was same after changing

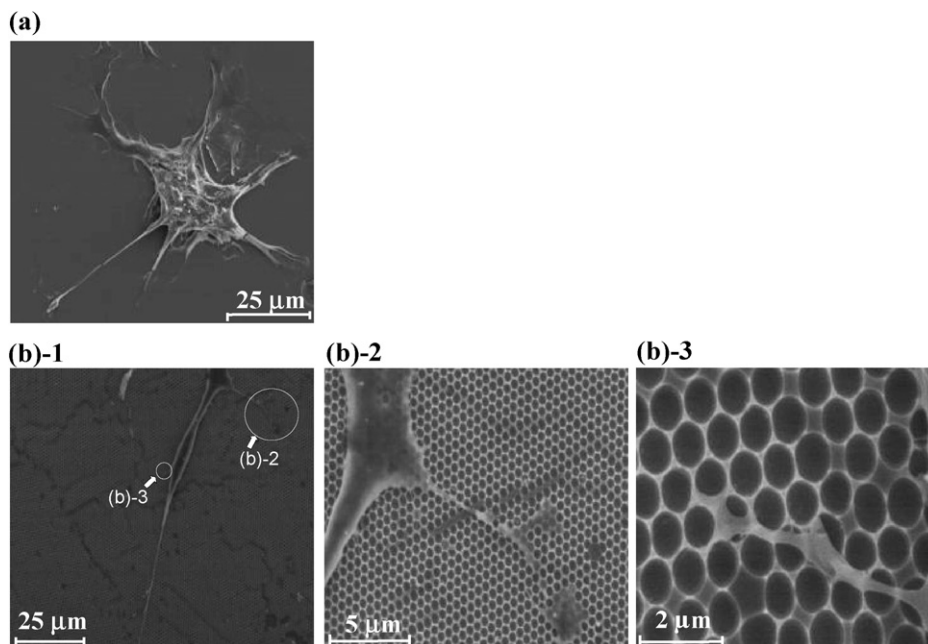


Fig. 7. SEM images of MC3T3-E1 cells cultured on (a) non-porous silica films and (b) silica films with a pore size of 1000 nm.

the hydrophilic balance of the surface of macroporous silica films.

To confirm the morphology of cells cultured on hydrophilic macroporous silica films, expression of actin filaments was analyzed (Fig. 10). The cells were elongated and actin stress fibers were virtually absent on amino-group-modified macroporous silica films. The average cell size observed on macroporous silica films was approximately  $4 \mu\text{m} \times 220 \mu\text{m}$ , which was smaller than the average cell size observed on non-porous silica films, which was approximately  $30 \mu\text{m} \times 40 \mu\text{m}$ .

Subsequently, similar changes were found in the proliferation and morphology of cells regardless of amino functionalization of macroporous silica films. These findings indicate that the contact angle determined by the balance of hydrophilicity and hydrophobicity of the macroporous films does not affect cell behavior; this unique phenomenon has not been reported until now. Indeed, Hertz et al. [34] reported that hydrophobic, but not hydrophilic, statins enhance phagocytosis and decrease apoptosis in human peripheral blood cells. The present study suggests that cell proliferation and morphology are strictly dependent on the surface size of the macroporous silica films.

#### 3.4. Cell behavior on HAp and alumina macroporous films

Fig. 11(1) and (2) shows cell viability and proliferation on HAp and alumina macroporous films. The initial number of cells attached to each film after 24 h of culturing was shown to be almost equal. Even after 72 h, no dead cells were observed after staining the HAp films with propidium iodide (PI). The proliferation rate of MC3T3-E1 cells on HAp films with a pore size of 1000 nm increased by approximately 20% compared to that of cells on non-porous HAp films. These results indicate that after 72 h of culturing on HAp films with a pore size of 1000 nm, cell growth was controlled by not only the macroporous film structure but also its material properties.

On the other hand, cell numbers after 72 h of culturing decreased by approximately 72% and 34% on alumina films with pore sizes 500 and 1000 nm, respectively, and that some dead cells were observed on films of the same pore sizes [Fig. 11(1)-(d) and (e) and (2)].

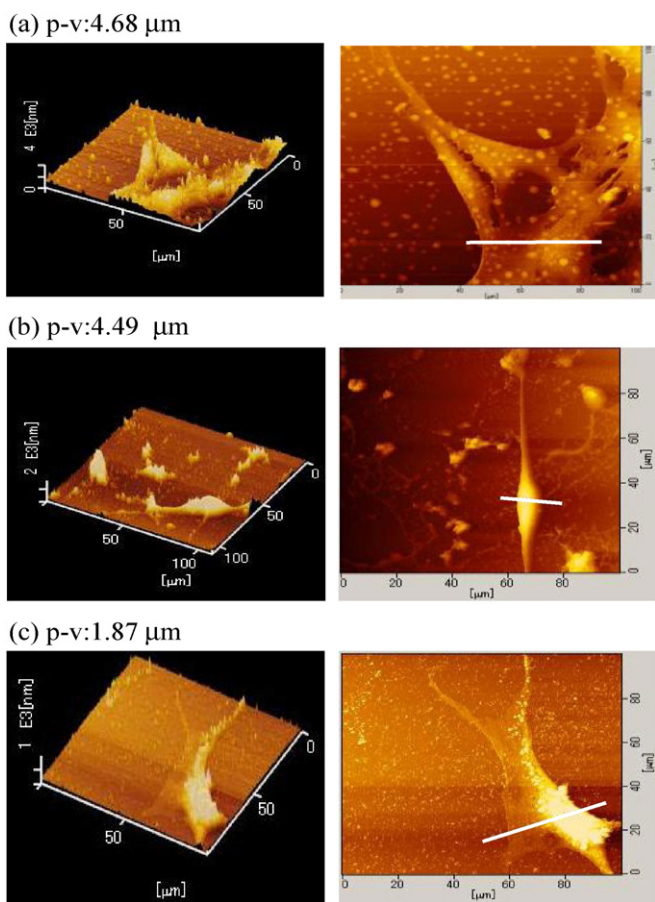
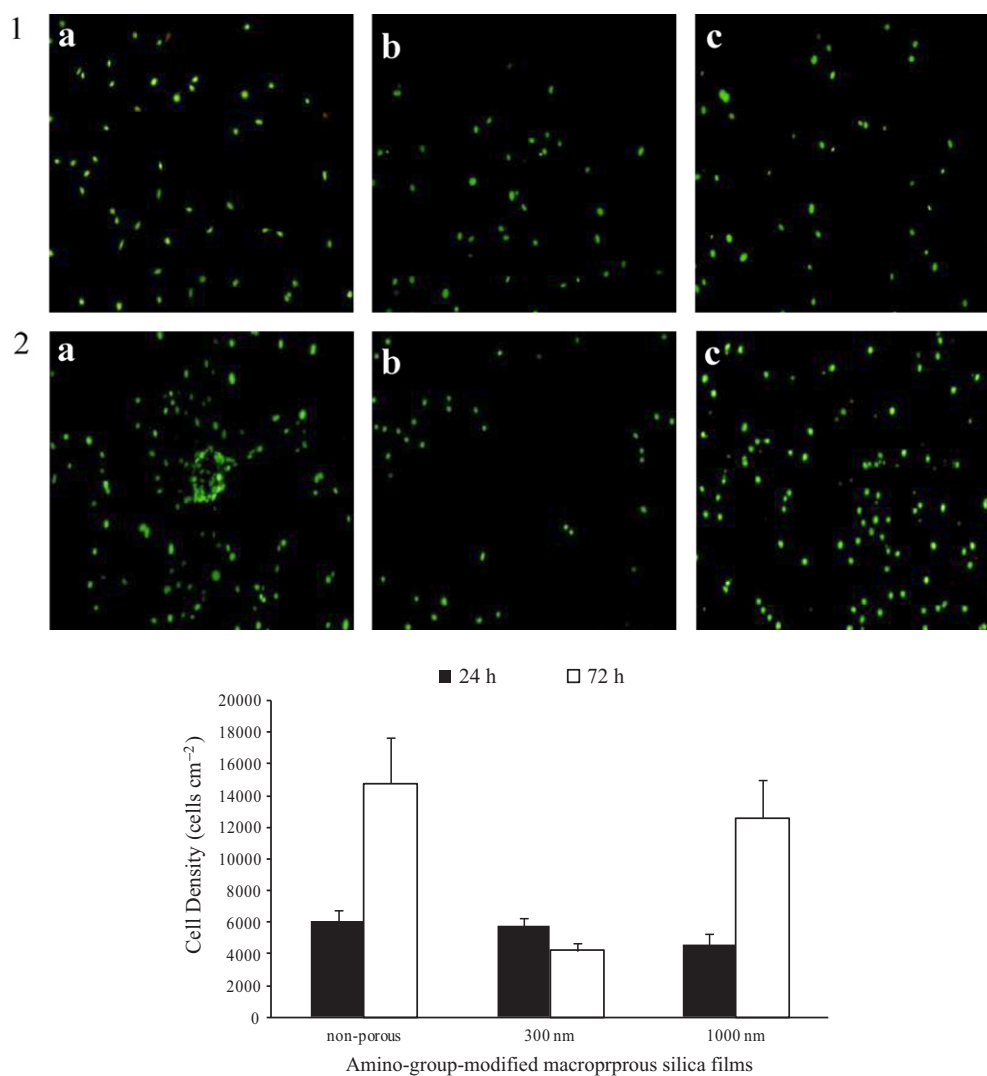


Fig. 8. Typical SPM images of the cells on (a) non-porous silica films, (b) silica films with a pore size of 100 nm, and (c) cover-slip. The p-v value of each substrate indicates the maximum difference in height, as indicated on the white line.



**Fig. 9.** (1) Evaluation of the adhered cell viability on amino-group-modified macroporous silica films by staining with Cyto dye, a cell-permeable green fluorescent dye for live cells, and propidium iodide (PI), a non-cell-permeable red fluorescent dye for dead cells. Cell culture was performed for 24 h (A) and 72 h (B). (a) Non-porous silica films, (b) pore size 300 nm, and (c) pore size 1000 nm. (2) MC3T3-E1 cells proliferation cultured on amino-group-modified macroporous silica films. After the cells were stained by the same method as described in Section 2.4, cell numbers (density), which are represented as values per unit area were evaluated using ImageJ software. The error bars indicate the standard deviation ( $n = 3$ ). A pore size of 300 nm resulted in a significantly decreased cell density compared with the non-porous films; however, a pore size of 1000 nm resulted in a similar cell density as compared with the non-porous films.

The cell proliferation rate obtained on alumina films was almost equal to that observed on silica films. The differences in cell proliferation rates on silica, HAp, and alumina films reveal that cell growth is relatively regulated by the characteristics of each constituent used in macroporous scaffolding. Macroporous HAp films

did not have an effect on restraining cell proliferation that was recognized on macroporous silica and alumina films. HAp is known to be highly compatible with MC3T3-E1 cells, and therefore, a higher number of focal adhesions were formed and cell proliferation was promoted.

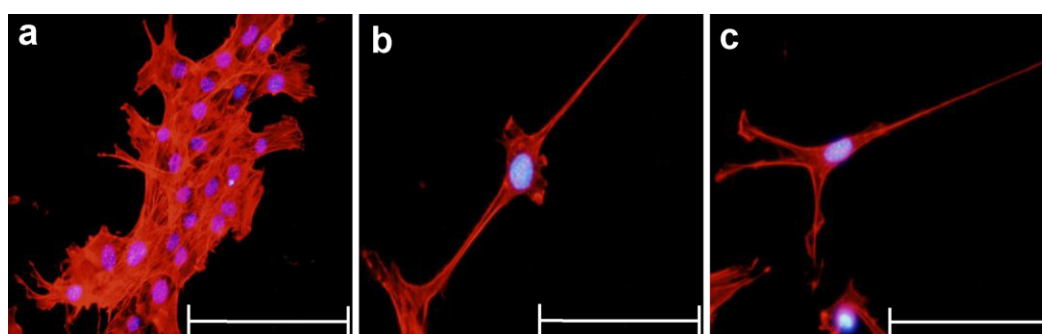


**Fig. 10.** Fluorescent microscopic images of F-actin of cells adhered to amino-group-modified macro porous silica substrates. Cell nuclei are immunostained in blue and actin fibers are stained in red. (a) Non-porous silica films, (b) 300 nm pores, and (c) 1000 nm pore size. Scale bar: 100  $\mu\text{m}$ . (For interpretation of the references to color in this text, the reader is referred to the web version of this article.)

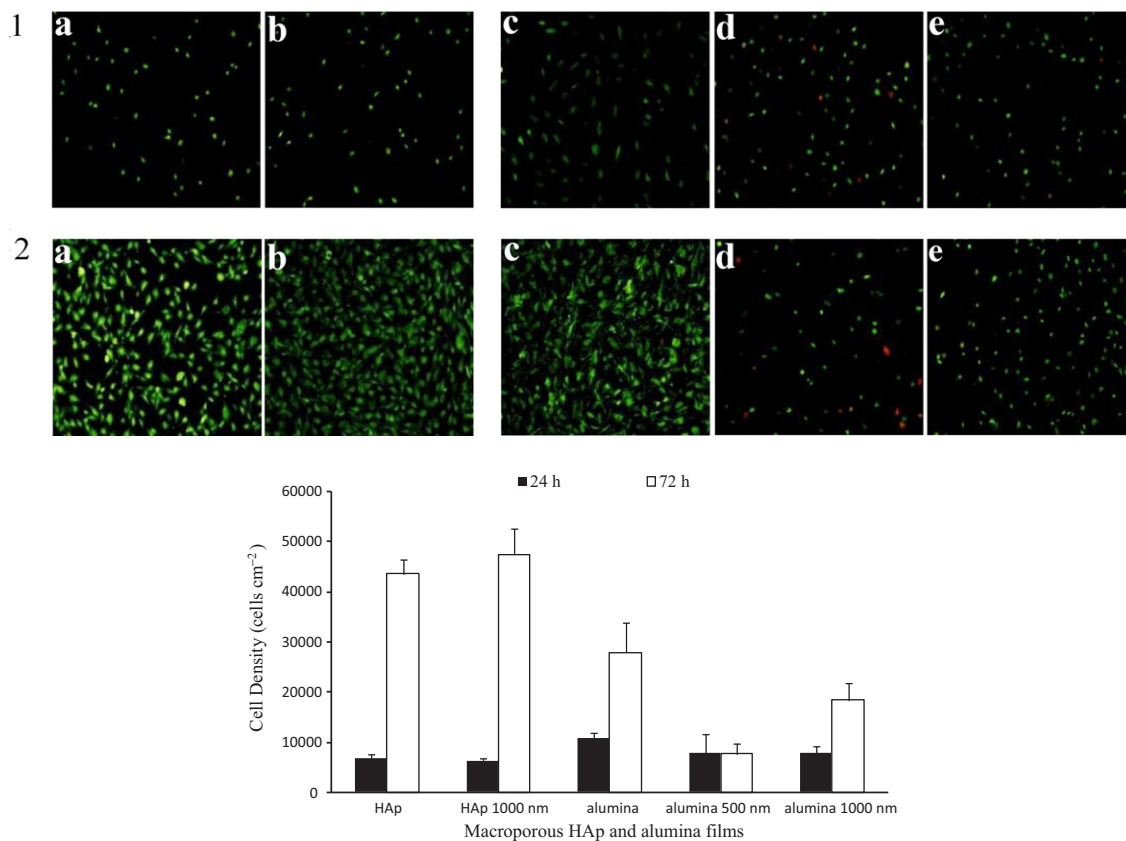


**Fig. 11.** (1) Evaluation of adherent cell viability on macroporous HAp and alumina films by staining with Cyto dye, a cell-permeable green fluorescent dye for live cells, and propidium iodide (PI), a non-cell-permeable red fluorescent dye for dead cells. Cell culture was performed for 24 h (A) and 72 h (B). (a) Non-porous HAp films, (b) HAp films with a pore size of 1000 nm, (c) non-porous alumina films, (d) alumina films with a pore size of 500 nm, and (e) alumina films with a pore size of 1000 nm are shown. (2) MC3T3-E1 cells proliferation cultured on macroporous HAp and alumina films. After the cells were stained by the same method described in Section 2.4, cell numbers (density), which are represented as values per unit area were evaluated using ImageJ software. The error bars indicate the standard deviation ( $n = 3$ ).

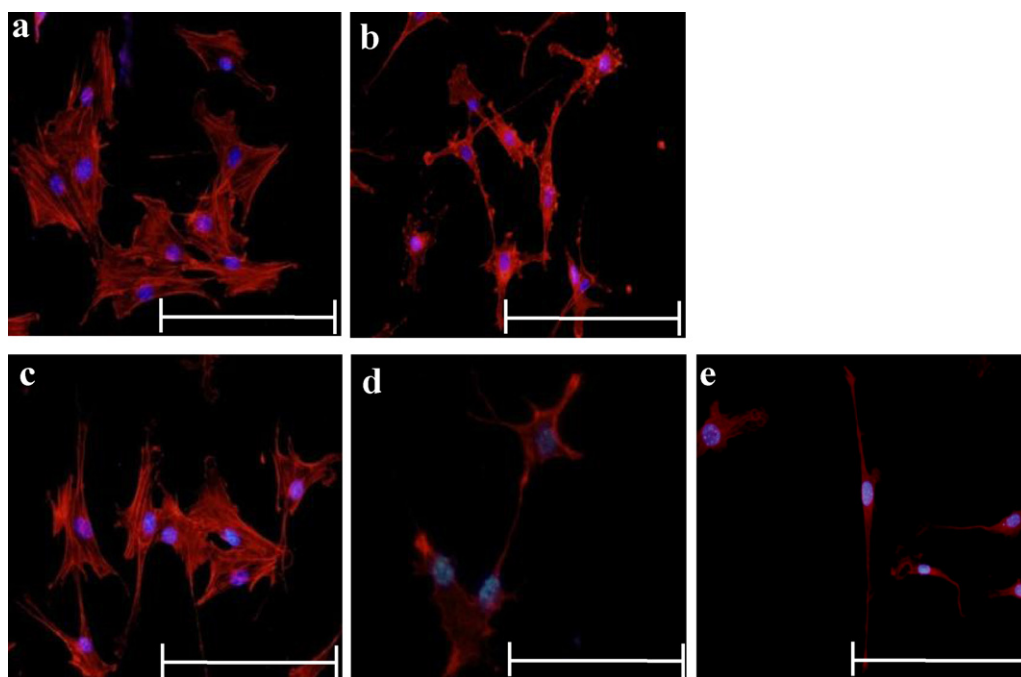


**Fig. 12.** Fluorescent microscopic images of F-actin of cells adhered to HAp and alumina films. (a) Non-porous HAp films, (b) HAp films with a pore size of 1000 nm, (c) non-porous alumina films, (d) alumina films with a pore size of 500 nm, and (e) alumina films with a pore size of 1000 nm are shown. Scale bar: 100 μm.

To confirm the influence of different compositions, analysis of the actin filaments were performed. Cells were uniaxially elongated on macroporous HAp and alumina films [Fig. 12(b), (d) and (e)], whereas cells on non-porous HAp and the alumina films spread out in multiple directions [Fig. 12(a) and (c)]. Cell sizes on macroporous HAp and alumina films were approximately  $15\ \mu\text{m} \times 40\ \mu\text{m}$  and those on non-porous HAp and alumina films were approximately  $30\ \mu\text{m} \times 60\ \mu\text{m}$ .

#### 4. Conclusions

Controlling cellular behavior on biomaterials is necessary for the development of tissue scaffolds, biomedical implants, and drug delivery devices. This study, specifically focused on the effects of pore size and the inorganic composition of macroporous films prepared using the inverse-opal method on cell proliferation and morphology. The proliferation of osteoblast-like MC3T3-E1 cells was significantly restricted by macroporous silica films with 100 nm, 300 nm, and 500 nm pore sizes. However, when macroporous silica with a pore size of 1000 nm was employed, only a slight restriction on cell proliferation was observed. Even the amino-group-modified hydrophilic macroporous silica films had similar results, the same inhibitory effect on cell growth was detected. In case of macroporous HAp films, the number of growing cells steadily increased. The number of actin stress fibers decreased on macroporous silica, HAp, and alumina films compared to non-porous silica, HAp, and alumina films. In addition, MC3T3-E1 cells on non-porous films exhibited a high degree of multi directional spread and showed a highly flattened morphology. Their shapes, however, became similar to fibroblast cells when they were cultured on macroporous films.

One of the critical points of the present study is that nanoscale pore size and the composition of the scaffolding affects cell proliferation. Moreover, it was found that macroporous film can potentially control the morphology of MC3T3-E1 cells. These results provide important information for use in tissue engineering and regenerative medicine that could be applied to the development of new artificial blood vessel surfaces and cell culture dishes. Additional studies on differentiation and osteoblast-specific gene expression of cells on macroporous films are currently in progress.

#### References

- [1] K. Anselme, *Biomaterials* 21 (2000) 667.
- [2] A. Kikuchi, T. Okano, *J. Control. Release* 101 (2005) 69.
- [3] A. Thapa, D.C. Miller, T.J. Webster, K.M. Haberstroh, *Biomaterials* 24 (2003) 2915.
- [4] X.L. Zhu, J. Chen, L. Scheideler, R. Reichl, J. Geis-Gerstorfer, *Biomaterials* 25 (2004) 4087.
- [5] J. Tan, W.M. Saltzman, *Nat. Mater.* 6 (2007) 997.
- [6] M.J. Dalby, S. Childs, M.O. Riehle, H.J.H. Johnstone, S. Affronssman, A.S.G. Curtis, *Biomaterials* 24 (2003) 927.
- [7] M.J. Dalby, D. Giannaras, M.O. Riehle, N. Gadegaard, S. Affronssman, A.S.G. Curtis, *Biomaterials* 25 (2004) 77.
- [8] J. Park, S. Bauer, P. Schmuki, K.V.D. Mark, *Nano Lett.* 9 (2009) 3157.
- [9] E. Martineza, E. Engelb, J.A. Planell, J. Samitier, *Ann. Anat.* 191 (2009) 126.
- [10] J.P. Spatz, B. Geige, *Method Cell Biol.* 83 (2007) 89.
- [11] N.R. Washburn, K.M. Yamada, C.G. Simon Jr., S.B. Kennedy, E.J. Amis, *Biomaterials* 25 (2004) 1215.
- [12] P.T. Ohara, R.C. Buck, *Exp. Cell Res.* 121 (1979) 235.
- [13] R.G. Flemming, C.J. Murphy, G.A. Abrams, S.L. Goodman, P.F. Nealey, *Biomaterials* 20 (1999) 573.
- [14] A. Itala, H.O. Ylanen, J. Yrjans, T. Heino, T. Hentunen, M. Hupa, *J. Biomed. Mater. Res.* 62 (2002) 404.
- [15] M. Nitschke, G. Schmack, A. Janke, F. Simon, D. Pleul, C. Werne, *J. Biomed. Mater. Res.* 59 (2002) 632–638.
- [16] M.H. Wu, C. Park, G.M. Whitesides, *J. Colloid Interface Sci.* 265 (2003) 304.
- [17] T. Saito, H. Hayashi, T. Kameyama, M. Hishida, K. Nagai, K. Teraoka, K. Kato, *Mater. Sci. Eng. C* 30 (2010) 1.
- [18] D.E. Ingber, *Proc. Natl. Acad. Sci. U.S.A.* 87 (1990) 3579.
- [19] K.L. Prime, G.M. Whitesides, *Science* 252 (1991) 1164.
- [20] R. Vaidya, L.M. Tender, G. Bradley, M.J. O'Brien II, M. Cone, G.P. Lopez, *Biotechnol. Progr.* 14 (1998) 371.
- [21] D. Motlagh, T.J. Hartman, T.A. Desai, B. Russell, *J. Biomed. Mater. Res. A* 67 (2003) 148.
- [22] D. Motlagh, S.E. Senyo, T.A. Desai, B. Russell, *Biomaterials* 24 (2003) 2463.
- [23] Y. Fukuhira, H. Kaneko, M. Yamaga, M. Tanaka, S. Yamamoto, M. Shimomura, *Colloids Surf. A* 313–314 (2008) 520.
- [24] M. Sakurai, A. Shimojima, M. Heishi, K. Kuroda, *Langmuir* 23 (2007) 10789.
- [25] F. Meseguer, A. Blanco, H. Miguez, F. Garcia-Santamaria, M. Ibisate, C. Loipez, *Colloids Surf. A* 202 (2002) 281.
- [26] D. Nagao, R. Kameyama, H. Matsumoto, Y. Kobayashi, M. Konno, *Colloids Surf. A* 317 (2008) 722.
- [27] S. Madhavi, C. Ferraris, T.J. White, *J. Solid State Chem.* 178 (2005) 2838.
- [28] Q. Yuan, A.X. Yin, C. Luo, L.D. Sun, Y.W. Zhang, W.T. Duan, H.C. Liu, C.H. Yan, *J. Am. Chem. Soc.* 130 (2008) 3465.
- [29] A.M. Lipski, C.J. Pino, F.R. Haselton, I.W. Chen, V.P. Shastri, *Biomaterials* 29 (2008) 3836.
- [30] A. Alberts, A. Johnson, J. Lewis, M. Raff, K. Roberts, P. Walter, *Molecular Biology of the Cell*, 4th edn., Garland Science, New York, 2002.
- [31] A.S.G. Curtis, N. Gadegaard, M.J. Dalby, M.O. Riehle, C.D.W. Wilkinson, G. Aitchison, *IEEE Trans. Nanobiosci.* 3 (2004) 61.
- [32] M.J. Dalby, D. McCloy, M. Robertson, H. Agheli, D. Sutherland, S. Affrossman, R.O.C. Oreffo, *Biomaterials* 27 (2006) 2980.
- [33] J. Park, S. Bauer, K. Mark, P. Schmuki, *Nano Lett.* 6 (2007) 1686.
- [34] S. Hertz, B. Michael, D. Meir, B. Hanna, *Biomed. Pharmacother.* 62 (2008) 41.